Fatty Ethanolamide of Bertholletia Excelsa Triglycerides (Brazil nuts): Anti-Inflammatory Action and Acute Toxicity Evaluation in Zebrafish (Danio rerio)

Yesica Fernanda Quitian-Useche
Universidade Federal do Amapa
Brenda Lorena Sánchez-Ortiz
Universidade Federal do Amapa
Swanny Ferreira Borges
Universidade Federal do Amapa
Benilson Ramos
Universidade Federal do Amapa
Gisele Custódio de Souza
Universidade Federal do Amapa
Mateus Alves Batista
Universidade federal do Amapa
Lorane Izabel da Silva Hage-Melim
Universidade Federal do Amapa
Irlon Maciel Ferreira
Universidade Federal do Amapa
Jose Carlos Tavares Carvalho (jctcarvalho@gmail.com)
Universidade Federal do Amapá https://orcid.org/0000-0003-3662-9794
Raphaelle Sousa Borges
Universidade Federal do Amapa

Research Article

Keywords: N-alkylamide, Bertholletia excelsa oil, anti-inflammatory, zebrafish

Posted Date: June 4th, 2021

DOI: https://doi.org/10.21203/rs.3.rs-437833/v1

Abstract

Fatty amides (*N*-alkylamides) are a group of bioactive lipids widely distributed in microorganisms, animals, and plants. The low yield in the extraction process of spilantol, a grease amide, which has been related mainly to diverse biological effects, compromises its application on a large scale. Thus, this study proposed an alternative to the synthesis of fatty amides from *Bertholletia excelsa* (AGBe) oil, with a chemical structure similar to that of spilantol. In vivo models induced by carrageenan were used in Zebrafish (*Danio rerio*). In in vivo studies, oral AGBe produced no signs of toxicity. In the histopathological study, AGBe did not cause significant changes in the main metabolizing organs (liver, kidneys, and intestines). In the anti-inflammatory evaluation, all doses (45 mg/kg, 500 mg/kg, and 1000 mg/kg) were effective, significantly reducing edema and producing a dose-response effect when compared to spilantol. In the *in silico* study, with the use of molecular docking, he showed that among the AGBe, the molecules 18:1, ω-7-ethanolamine and 18:1, ω-9-ethanolamine stood out, which had 21 interactions for COX-2 and 20 interactions for PLA_2, respectively, surpassing the spilantol standard with 15 interactions for COX-2 and PLA_2. The hypothesis of anti-inflammatory action was confirmed in the *in silico* study, demonstrating the involvement of AGBe in the process of inhibiting the enzymes COX-2 and PLA_2. Therefore, based on all the results obtained and the fact that until the dose of 1000 mg/kg, orally, in zebrafish, it was not possible to determine the LD_{50}, it can be said that AGBe is effective and safe for the activity anti-inflammatory.

Introduction

Ethnopharmacological studies are being conducted more and more due to the growing demand worldwide for new drugs and, the chemical components present in medicinal plants have been associated with several pharmacological effects. Therefore, natural resources have been considered important to raise health and quality of life (Shawahna et al. 2017).

Among the biologically active components, but reported and found in medicinal plants, we highlight the fatty amides found in abundance in *Bertholletia excelsa*, a tree of the Lecythidaceae family, also known as chestnut from Pará or Brazil. It is a species native to the Amazon region, considered one of the main riches of the Amazon jungle, being the most exported raw material in the region. The oil extracted from the seed of *Bertholletia excelsa* has stood out for presenting high nutritional value and several biological activities such as healing, antioxidant, and anti-inflammatory (Chunhieng et al. 2008; Muniz et al. 2015).

In this context, the species *Acmella oleracea* is found, a plant belonging to the Asteraceae family, found mainly in the northern region of Brazil, where it is usually used in local cuisine and popularly known as Jambú (Dos Santos, 2015). The active compound found in greater abundance in this plant is spilantol (*N*-Alkylamide), a grease amide with the chemical formula ($C_{14}H_{23}NO$, 221.339 g/mol) (Molina Torres et al. 1996; Barbosa *et al*. 2015). Spilantol has stood out in scientific studies that demonstrate its relationship with several biological effects, such as analgesic, neuroprotective, anticonvulsant, antioxidant, and anti-inflammatory (Wu et al. 2008; Hernández et al. 2009; Dias et al. 2011; Da Silva, 2013).

Among the various symptoms, inflammation is a warning sign for the body, and the prolongation of the inflammatory process can cause damage to cells and tissues. However, most of the commercialized anti-inflammatory drugs cause adverse reactions when used in the long term. Considering ethnopharmacology and ethnomedicine, some products of natural origin have been studied and pointed out as possible alternative drugs for the treatment of inflammation. This has been one of the biggest challenges for doctors and pharmacists who develop research with products of natural origin (García De Lorenzo et al. 2000; Shawahna et al. 2017; Carvalho, 2017).

Carrying out this study, zebrafish (*Danio rerio*) was selected as an animal model, as it has been recognized pharmacologically for its advantages in carrying out scientific research and validating new drugs, and this animal species has been successfully applied in the pharmaceutical area (Hsu et al. 2007; Chakraborty et al. 2010; Schmidt et al. 2013; Kettleborough et al. 2013; Peterson et al. 2015; Burgan, 2016; Carvalho et al. 2017; Borges et al. 2018).

Given the above, the present study proposed obtaining fatty amides from *Bertholletia excelsa* oil and its pharmaco-toxicological validation for anti-inflammatory activity in zebrafish (*Danio rerio*), using spilantol, a grease starch extracted from the flowers of *Acmella oleracea* proven to be effective against the inflammatory process.

Materials And Methods

Plant material - obtaining spilantol

Spilantol was previously obtained in a study by Souza et al. (2019) from the plant species *Acmella oleracea*, and in this study, it was used as an anti-inflammatory standard for fatty amides from *Bertholletia excelsa* oil.

Obtaining fatty amides (*N*-alkylamides) from *Bertholletia excelsa* oil

Bertholletia excelsa oil was purchased from the Mixed Vegetable Extractive Cooperative of Laranjal do Jari Farmers (COMAJA Co.), Municipality of Laranjal do Jari, Amapá, Brazil. They were stored at -4 ºC until the moment of use. Ethanolamine (99.5%), Amano lipase from *Pseudomonas fluorescens* [LPF (20.000 U/g, CAS 9001-62-1)] e hexane (98%) were purchased from Synth Co. (São Paulo, Brazil).

The amidation reaction (Figure 1) was carried out with ethanolamine (6.0 mL) and BNO (2.0 mL) and 10% LPF (w/w of chestnut oil) as a catalyst, remaining in magnetic stirring for 24 h (300 rpm, 50 ± 2 °C). After that period, the enzyme was filtered, and the filtrate was extracted with dichloromethane (3 × 25 mL). The organic phase was dried over anhydrous Na_2SO_4, filtered, and evaporated under reduced pressure. Finally, the expected products were purified by column chromatography with silica gel and a mixture of n-hexane: ethyl acetate (8: 2) as an eluent (Barata et al., 2020).

GC-MS analysis

Fatty acids and fatty amides from *Bertholletia excelsa* oil were characterized by gas chromatography coupled to mass spectrometry (GC-MS), was performed on a Shimadzu/GC 2010 apparatus coupled to a Shimadzu/AOC-5000 autoinjector and an electron beam impact detector (Shimadzu MS2010 Plus) (70 eV), equipped with a DB-5MS fused silica column (Agilent J & WAdvanced 30 m x 0.25 mm x 0.25 mm) (65 kPa). The parameters used were; 1:15 split ratio, helium as the carrier gas, injection volume of 1.0 mL, injector temperature of 250 °C, detector temperature of 270 °C, initial column temperature of 100 °C for 2 min, rate of heating from 6 ºC min^{-1} to 280 ºC for 5 min. The total analysis time was 37 min. The identification of fatty acid amides was made by comparing the fragmentation spectrum with those in the GC-MS library (MS database, NIST 5.0) (Araújo et al., 2018).

Identification of fatty amides

Spectroscopic profile in the infrared region

Obtaining the spectroscopic profile in the infrared region, the samples (chestnut oil and fatty amides) were impregnated in KBr tablets, and the sample readings were performed on an Infrared Spectrometer by Fourier transform (FTIR) (Shimadzu IR Prestige -21), with a wavelength of 400 to 4000 cm^{-1} with a resolution of 4 cm^{-1} with 64 scans.

Animal experimentation

Animals

180 units of zebrafish (*Danio rerio*) of the wild strain from Aqua New Aquários e Peixe Ltda. ME (PE, Brazil) following the methodology of Souza et al. (2016) and Borges et al. (2018) were used. The experiments were carried out following the rules established for the care of animals, and the project was approved by the Ethics Committee on the Use of Animals - CEUA - UNIFAP, of the Federal University of Amapá with protocol number 020/2019.

Determination of the average lethal dose (LD_{50}) and behavioral assessment

To obtain the average lethal dose (LD_{50}), after treatment, the animals were observed for 48 hours. In this test, adult zebrafish (standard length of 28.1 ± 0.2 mm weighing 0.42 ± 0.04 g) was used. The animals were treated orally through gavage, as described by Carvalho et al. (2017) and Borges et al. (2018). The doses of AGBe administered were: 45 mg/kg, 500 mg/kg, and 1000 mg/kg, based on previous studies by Souza et al. (2019).

Each dose of AGBe was evaluated in groups of four animals; the tests were performed in triplicate, totaling 48 animals (n = 12 per group) distributed in the following groups: group A - vehicle - Thinners (Tween, DMSO, and distilled water) used to solubilize AGBe; group B - AGBe at a dose of 45 mg/kg; group C - AGBe at a dose of 500 mg/kg; group D - AGBe at a dose of 1000 mg/kg; group E - oil of *Bertholletia*

excelsa at a dose of 1000 mg/kg. Behavioral parameters were assessed as described by Souza et al. (2016) and Borges et al. (2018).

Carrageenan-induced abdominal edema assay

Carrageenan (iota type II, Sigma Co, Lot 65H1096) was applied intraperitoneally (i.p) in a volume of 20 µL (200 µg) in PBS, according to the methodology described by Borges et al. (2018), one h before the oral administration (v.o) of AGBe. The trial was performed in triplicate, and the doses of AGBe were selected from the toxicity trial and based on previous studies (Collymore et al. 2013; Carvalho et al. 2017; Borges et al. 2018).

The animals were divided into the following groups with n = 16 / group: **group A** - PBS: PBS-phosphate buffered saline (20 µl, i.p), substance used to solubilize carrageenan, and saline solution (2 µl, v.o); **group B** - Thinners: carrageenan (i.p) and solution used to dilute AGBe, (Tween - DMSO and distilled water, 2 µl, v.o); **group C** - indomethacin: carrageenan (i.p) and Indomethacin (10 mg / kg, v.o, Sigma Co. São Paulo, Brazil); **group D** - E (35 mg/kg): carrageenan (i.p) and spilantol at a dose of 35 mg/kg, v.o); **group E** - A (100 mg/kg): carrageenan (i.p) and AGBe at a dose of 100 mg/kg (v.o); **group F** - A (500 mg/kg): carrageenan (i.p) and AGBe at a dose of 500 mg/kg (v.o); **group G** - A (750 mg/kg): carrageenan (i.p) and AGBe at a dose of 750 mg/kg (v.o).

Histopathological study

At the end of the toxicological and inflammatory evaluation experiments, the animals were euthanized according to the recommendations of the American Guidelines of the Veterinary Medical Association for Animal Euthanasia (Leary et al. 2013), and the tissues were collected for the histopathological study.

For histopathological analysis, tissue preparation and microscopic analysis of the organs analyzed were based on the techniques described by Souza et al. (2016), Carvalho et al. (2017), and Borges et al. (2017). The Histological Changes Index (IHA) was calculated from the levels of tissue changes observed in the liver, kidneys, and intestines according to Borges et al. (2018) and Souza et al. (2019).

Statistical analysis

For determining the median lethal dose (LD_{50}), probit analysis was used using the GraphPad Prism software version 6.0. The results of the histopathological study were expressed as mean ± SEM and analyzed by ANOVA, followed by the Tukey-Kramer test for comparisons between the treated and control groups. Results with $p < 0.05$ were considered statistically significant. In evaluating anti-inflammatory activity, data were expressed as mean ± standard deviation, and the results were analyzed using the GraphPad Prism software version 8.0 using ANOVA (one-way), followed by the Tukey-Kramer post hoc test. Values of $p < 0.05$ were considered statistically significant.

Molecular docking of amides in biological targets related to the inflammatory process

For the docking study, files were deposited in the Protein Data Bank (PDB) of the Research Collaboratory for Structural Bioinformatics (Li et al. 2008; Sandy and Butler 2009; Orlando and Malkowski 2016) with the coordinates of the crystallographic structures of COX-1 therapeutic targets (PDB ID: 3N8X, resolution: 2.75 Å) complexed with the nimesulide inhibitor. COX-2 (PDB ID: 5IKQ, resolution: 2.41 Å) was complexed with meclophenamic acid and phospholipase A2 (PDB ID: 5G3N, resolution: 1.8 A Å) with 3- (5'-benzyl-2'-carbamoyl-biphenyl-3-yl) propanoic acid inhibitor.

The GOLD (Genetic Optimization for Ligand Docking) program uses the genetic algorithm for flexible ligand docking experiments within protein binding sites. The GOLD program was used to investigate the modes of interaction between the studied compounds and therapeutic targets (Chandak et al. 2014).

Performing molecular coupling, hydrogen atoms were added, and the water molecules of the enzymes were removed. Inhibitors that were complexed with each therapeutic target were extracted. Before performing the docking simulation, the results were validated by calculating the mean quadratic deviation (RMSD) between the experimental ligand and the conformation of the ligand that produced the best pose after docking.

The docking was calculated following the coordinates: cyclooxygenase-1 (COX-1): x: -21.44, y: -50.78 ez: 1.42 and a radius of 10 Å; cyclooxygenase-2 (COX-2): x: 22.83, y: 51.56, and z: 17.81 and a radius of 9 Å; and phospholipase A2 (PLA_2): x: 7.48, y: 3.41 and z: -0.16 and a radius of 9 Å. identifying the interactions between the compounds and the therapeutic targets, it was necessary to identify the amino acids that make up the catalytic site of the enzymes: COX-1 (ARG120, TYR355, ILE523, and SER530), COX-2 (TYR385 and SER530) (Borges et al. 2017) and PLA2 (PHE5 and ILE9) (Giordanetto et al. 2016).

Results

Infrared and CG - MS analysis

In the spectrum in the infrared region, the amides present (Figure 2) a band in 3294 cm^{-1} originated by stretching vibrations of the N-H bond; in 2918 and 2848 cm^{-1} referring to the asymmetric and symmetrical C-H stretch respectively; at 1643 cm^{-1}, an amide group C = O absorption band; in 1558 cm^{-1} folding band N-H of secondary amides; At 1468 cm^{-1} was observed bands of vibrations of asymmetric angular deformation of the C-H connections of the aliphatic groups.

In the infrared spectrum of the oil of *Bertholletia excelsa* (Figure 2), it is possible to observe bands in the region of 3007 cm^{-1} referring to the stretch = -CH; in 2929 and 2854 cm^{-1} referring to the asymmetric and symmetrical C-H stretch respectively; in 1747 cm^{-1} for the C = O stretch and in 1163 cm^{-1} for the C-O ester stretch. At 1462 cm^{-1} and 1377 cm^{-1}, the bands of vibrations of asymmetric angular deformation of the C-H connections of the aliphatic groups can be seen.

Oleic acid (C18:1, Δ-9) is the major fatty acid contained in the *Bertholletia excelsa* oil with 32%, followed by polyunsaturated linoleic acid (C18:2, Δ-6) (29%) and vaccenic acid (C18:1, Δ-7) to a lesser extent at 2%.

Other fatty acids identified in this oil sample were palmitic acid (C16:0; 19%) followed by stearic acid (17%). In (Table 1) profile of fatty acid in the *Bertholletia excelsa* oil is shown, which is accord to the reported by Barata et al. (2020).

The triglyceride characterization by IR spectroscopy of Brazil nut oil, Figure x, shown a peak in 3001 cm^{-1} corresponds to the stretching of the $-C-H_{(sp2)}$ and 2933 and 2860 cm^{-1} to the stretching of the ligation $-C-H_{(sp3)}$. Signals of the amidated compound are listed as the peaks in 3313 cm^{-1} which correspond to the stretch –NH, and the peak in the 1644 and 1556 cm^{-1} correspond to the folding of the ligation –N–H, characteristics of the fatty amide synthesized. Another showed a powerful signal at 1746 cm^{-1} for the C=O stretching ester vibration; this signal is shifted to a lower frequency at 17633 cm^{-1} for fatty amide.

The fatty amides from ethanolamine were characterized by MS spectrum with a typical base peak at *m/z* 116 (for *N*-(2-hydroxyethyl)oleamide), resultants from McLaffery rearrangement and γ-cleavage, respectively (Figure 2). In contrast, observations for the ethyl oleate structure mass spectra (Figure 3) presented the m/z 55 fragmentation ion as the base peak and was less abundant than the ion related to the loss of the ethoxide portion (*m/z* 264).

Obtaining the average lethal dose (LD_{50})

The animals treated with AGBe and oil of *Bertholletia excelsa* did not die during and after the experiment, including those treated with the highest dose (1000 mg/kg, v.o). The animals show stressful behavior in the first hours, and soon, they recovered. In the histopathological evaluation, it was observed that both AGBe and *Bertholletia excelsa* oil did not produce tissue damage that could alter the functioning of the main organs (Figure 4). Also, *Bertholletia excelsa* oil demonstrated liver toxicity (Figure 5).

Molecular docking of amides in biological targets related to the inflammation process

The RMSD values obtained with the inhibitors nimesulide, meclofenamic acid, and 3- (5'-benzyl-2'-carbamoylbiphenyl-3-yl) propanoic acid were 0.835 Å; 0.535 Å and 0.978 Å for the respective therapeutic targets COX-1, COX-2 and PLA_2.

Docking between therapeutic targets and spilantol compounds, 16:0-ethanolamine, 18:2, ω-6-ethanolamine, 18:1, ω-9-ethanolamine, 18:1, ω-7-ethanolamine and 18:0-ethanolamine (Figure 12), with the highest score for the therapeutic target COX-1 (Figure 13), presented 14 interactions, being 13 hydrophobic and one conventional hydrogen interaction with the amino acids VAL116, ARG120, VAL349, LEU352, LEU359, TYR385, TRP387, PHE518, MET522, ILE523, and LEU531. The score observed for the best position was 72.86.

The grease amide 16:0-ethanolamine showed 13 interactions, 11 of which were hydrophobic and 2 of hydrogen with the amino acids HIS90, PRO191, LEU352, TYR385, TRP387, ASN515, PHE518, and ILE523. Para a melhor pose, foi observado o valor de 71,53 do escore.

For grease amide 18:2, ω-6-ethanolamine, 15 interactions were observed, 11 of which are hydrophobic and four hydrogen interactions with the amino acids HIS90, PRO191, GLN192, LEU352, TYR355, TRP387, ASN515, PHE518, ILE523, and ALA527. The score value obtained for the best position was 77.21.

The 18:1 grease amide, ω-9-ethanolamine showed 16 interactions, 14 of which were hydrophobic and two hydrogen interactions with the amino acids HIS90, GLN192, VAL349, LEU352, TYR355, LEU384, TRP387, ASN515, PHE518, ILE523, and ALA527. The observed score value was 71.76 for the best pose.

For the 18:1 amide, ω-7-ethanolamine, 16 interactions were identified, 15 of which in the hydrophobic category and one hydrogen interaction with the amino acids PRO86, VAL116, VAL349, LEU352, TYR355, PHE381, LEU384, TYR385, TRP387, PHE518, ILE523, and ALA527. The highest score value is observed at 78.40.

The grease amide 18:0-ethanolamine showed seven interactions, 6 of which were hydrophobic and 1 of hydrogen with the amino acids HIS90, LEU352, PHE518, MET522, and ILE523-having the score value for the best position of 74.41.

Considering the amino acids present in the active site, only spilantol interacted with the ARG120 residue. For the amino acid ILE523, all molecules interact. The amino acid residue TYR355 showed interaction with the molecules 18:2, ω-6-ethanolamine, 18: 1, ω-9-ethanolamine, and 18:1, ω-7-ethanolamine. However, no linker interacted with the amino acid residue SER530.

With the therapeutic target COX-2 (Figure 14), the spilantol and 18:2, ω-6-ethanolamine molecules showed 15 interactions, the first being 14 hydrophobic and a hydrogen interaction with the amino acids VAL116, VAL349, LEU352, TYR355, PHE381, LEU384, TYR385, TRP387, PHE518, MET522, VAL523, and LEU531, with a score of 63.00 for the best pose. Moreover, for the 18:2 molecule, ω-6-ethanolamine, 13 hydrophobic and two hydrogen interactions with the amino acids VAL116, VAL349, LEU352, TYR385, TRP387, PHE518, VAL523, ALA527, and LEU531, obtaining a score of 76.71.

For the 16:0-ethanolamine and 18:1, ω-9-ethanolamine molecules, 18 interactions were observed, with the first being 13 hydrophobic and five hydrogen interactions with the amino acids SER119, ARG120, VAL349, LEU352, TYR355, PHE381, LEU384, TYR385, TRP387, PHE518, MET522, VAL523, and ALA527, obtaining the score value of 75.21. For 18: 1, ω-9-ethanolamine, 15 hydrophobic and three hydrogen interactions with the amino acids VAL116, VAL349, LEU352, SER353, LEU384, TYR385, TRP387, PHE518, MET522, VAL523, ALA527, and LEU531, with a score of 80, 55.

The 18:1, ω-7-ethanolamine and 18:0-ethanolamine molecules showed the highest number of interactions, 21 and 20. For the first, 20 hydrophobic interactions and one hydrogen interaction were observed with the amino acid residues VAL116, VAL349, LEU352, TYR355, LEU359, LEU384, TRP387,

PHE518, MET522, VAL523, ALA527, SER530, and LEU531, with a value of score of 78.14. For 18:0-ethanolamine, 13 hydrophobic interactions and seven hydrogen interactions were identified with amino acid residues VAL116, GLN192, VAL349, LEU352, SER353, TYR355, LEU359, PHE518, VAL523, ALA527, and LEU531, obtaining a score value of 71, 16.

Considering the active site's amino acids, interactions of the spilantol molecules, 18:2, ω-6-ethanolamine, 16:0-ethanolamine, and 18:1, ω-9-ethanolamine, with the residue TYR385 were observed. Moreover, for the SER530 amino acid residue, only the 18:1 molecule, ω-7-ethanolamine, interacted. This last molecule is noteworthy because it has the most significant number of interactions and, even though it does not interact with the TYR385 residue, it did interact with a nearby residue, LEU384. The 18: 0-ethanolamine molecule showed no interactions with the amino acids of the active site.

With the therapeutic target PLA2 (Figure 15), the standard spilantol molecule showed 15 intermolecular interactions, 11 of which were hydrophobic and 4 of hydrogen interactions with the amino acids LEU2, PHE5, HIS6, ILE9, ALA17, CYS28, GLY29, VAL30, CYS44, HIS47, ASP48, LYS62 and PHE98 with a score value of 62.45.

All other studied molecules had a score value and number of interactions greater than the standard molecule. The 16:0-ethanolamine and 18:1, ω-7-ethanolamine molecules showed 17 interactions, being, for the first ten hydrophobic and seven hydrogen interactions with the amino acid residues LEU2, PHE5, ILE9, ALA17, CYS28, CYS44, HIS47, ASP48, LYS52, GLU55, and LYS62, with a score of 81.18. For the 18:1 amide, ω-7-ethanolamine, there were 14 hydrophobic interactions and three hydrogen interactions, with the amino acid residues LEU2, PHE5, HIS6, ALA17, CYS28, GLY31, CYS44, HIS47, TYR51, GLU55, LYS62, and PHE98, obtaining the score value of 86.51.

The 18:2 molecule, ω-6-ethanolamine showed 19 interactions, 12 of which are hydrophobic and seven hydrogen interactions, with the amino acids LEU2, PHE5, HIS6, ILE9, ALA17, CYS28, VAL30, GLY31, CYS44, HIS47, ASP48, LYS52, GLU55, and PHE98, obtaining a score value of 83.93.

With the 18:1 ω-9-ethanolamine molecule, 20 interactions can be observed, 12 of which are hydrophobic and 8 of hydrogen, with the amino acid residues LEU2, PHE5, HIS6, ILE9, ALA17, CYS28, VAL30, GLY31, CYS44, HIS47, ASP48, LYS52, and GLU55, with the highest score obtained for the studied molecules, 87.02.

For the 18:0-ethanolamine molecule, 15 interactions were observed, ten hydrophobic interactions, and five hydrogen interactions with the amino acids LEU2, PHE5, HIS6, ALA17, CYS28, GLY31, CYS44, HIS47, ASP48, and GLU55, with a score of value 85.25.

Considering the amino acids of the active site, all molecules interact with the PHE5 amino acid residue. For the ILE9 residue, only spilantol, 16:0-ethanolamine, 18:2, ω-6-ethanolamine, 18:1, and ω-9-ethanolamine showed intermolecular interactions. The 18:1 ω-9-ethanolamine molecule stands out for

the PLA_2 target with the highest score value and number of interactions and interacts with the two amino acid residues of the active site.

With COX-2, MMA presented nine interactions with amino acid residues VAL 344, TYR348, VAL349, TYR385, TRP387, MET522, GLY526/ALA527, and SER530. PMA had five interactions with the amino acid residues Tyr355, Trp387, Met522, Val 523, and Gly526/Ala527. IMA presented seven interactions with amino acid residues Val349, Leu352, Trp387, Met522, Gly526, and Ala527.

Discussion

Animals, when in contact with any toxic substance, whether of synthetic or natural origin, may present characteristics that indicate a possible toxic effect in the short or long term. According to Ribeiro (2013), these substances can trigger changes in the different systems and the behavior, causing even the death of the animal (Mathur et al. 2011).

According to Huang et al. (2014); Borges et al. (2018), and Souza et al. (2019), zebrafish, when in contact with foreign substances, adopt patterns of stress behavior, as occurred in this study, after the oral administration of AGBe, they did not cause damage to the tissue level of the organs analyzed in the histopathological study.

In the toxicity test, it was observed that *Bertholletia excelsa* oil and AGBe showed nontoxicity with oral treatment, even at the highest dose (1000 mg/kg), and it is not possible to determine the LD_{50}. A similar result was obtained by Barata et al. (2020), who reported reduced cell toxicity for fatty amides.

Souza et al. (2019) reported that even substances of natural origin that do not cause behavioral changes or death in the zebrafish could cause internal damage in this animal, altering the normal functioning of some organs. According to the parameters presented in studies carried out by Souza et al. (2016) and Borges et al. (2017), the rate of histopathological changes observed in this study for the kidneys and intestines of animals treated with AGBe and *Bertholletia excelsa* oil, characterized these organs as normal, as they did not present changes that compromised the homeostatic pattern of the organs.

In this study, the *Bertholletia excelsa* oil was not toxic to the liver, and the IHA was 0. This result reinforces the studies by Pawel et al. (2013) and Barata et al. (2020), who did not demonstrate toxicity to liver and kidneys in rats, also stated low cellular toxicity for fatty amides.

Carnovali et al. (2016) evaluated the action of fatty acid amides in zebrafish and demonstrated that they prevent the alteration of bone markers in a prednisolone-induced osteoporosis model in adult zebrafish scales, whereas their esterified forms do not. These data suggest that long-chain fatty acid amides are involved in regulating bone metabolism.

In this study, carrageenan was used as an inflammatory agent in a zebrafish model. Huang et al. (2014) validated the use of carrageenan as an inflammatory inducer in the zebrafish peritoneum and, they

observed that i.p. injection of carrageenan produced typical symptoms of inflammation, such as swelling, and upregulated MPO, a leukocyte marker, as well as the proinflammatory proteins TNF-α and iNOS. Also, they demonstrated that local injection of carrageenan into soft tissues induces acute inflammation and that known compounds with anti-inflammatory properties can modulate the inflammatory responses of carrageenan-injected adult zebrafish.

Thus, in the evaluation of AGBe on the inflammatory process triggered by carrageenan, the protocols of Huang et al. (2014); Carvalho et al. (2017); Borges et al. (2018) using intraperitoneal carrageenan to induce the formation of abdominal edema in zebrafish.

The participation of cyclooxygenase products (prostaglandins) in carrageenan edema, especially in the second phase, has already been described in several studies (Zaa et al. 2012; Motta et al. 2013; Huang et al. 2014; Carvalho et al. 2017: Borges et al. 2018; Barata et al. 2020). Also, the effect of non-steroidal anti-inflammatory drugs, such as indomethacin, as an inhibitor of prostaglandin synthesis via COX-1 inhibition and IL-6 production (Motta et al. 2013).

The administration of carrageenan intraperitoneally produced the formation of abdominal edema, which was more visible in animals treated with thinner/carrageenan (Figure 6B), and treatment with different doses of AGBe (100, 500, and 750 mg/kg) orally produced an inhibitory effect on carrageenan edema in a dose-response manner (Figure 8B). These results are in line with those described by Barata et al. (2020) for the amides obtained from triglycerides of *Bertholletia excelsa* oil, which demonstrated antiedematogenic activity at doses of 20 and 40 mg/kg, on rat paw edema by carrageenan.

Fiorucci et al. (2001) and Barata et al. (2020) described that fatty acid amides inhibit cyclooxygenase and lipooxygenase, which leads us to consider that the effect of AGBe in this study is also related to the inhibition of cyclooxygenase.

In this study, molecular docking was performed for AGBe and standard anti-inflammatory drugs. This computational method is currently widely used in obtaining new drugs (Du et al. 2016). It describes the molecules' mode of interaction at the enzyme or receptor site through specific fundamental interactions and predicts the binding affinity between protein-ligand complexes.

Spilantol was used as a standard in the *in silico* study to compare the results since it has a chemical structure similar to the studied molecules and presents a report in the literature of anti-inflammatory activity (Wu et al., 2008).

The RMSD value indicates the accuracy of the docking poses calculated by the GOLD fitting algorithm compared to the poses, determined experimentally, of a compound linked to a biological target. Therefore, the calculation of docking with RMSD less than 2 Å for a proper conformation is considered successful. Therefore, it has justified validity (Cole et al. 2005).

Prostaglandins are derived from arachidonic acid (AA) in a reaction catalyzed by COX, which can exist as COX-1 and COX-2. AA upon neopathological stimuli is released from the cell membrane. Inhibitors of this

enzyme will interfere in this reaction, and then the disease process begins. Recently, the involvement of COX-1 in cancer and inflammation was firmly established (Vitale et al. 2016; Hage-Melim et al. 2019).

Chunhieng et al. (2008) and Barata et al. (2020) confirmed that the polyunsaturated fatty acids present in the oil of *Bertholletia excelsa* have as precursors different fatty amides, which have anti-inflammatory properties, probably acting in the COX pathway, as was observed in this study. AGBe identified as 18: 1, ω-7-ethanolamine and 18: 1, ω-9-ethanolamine, present in vaccenic and oleic fatty acids, showed more significant interaction for COX-2 and PLA2, which stood out for presenting a score and number of interactions greater than the spilantol pattern, interacting with the amino acids present in the active site or, at least, close to it in all the studied targets (Figure15, 16 and 17).

The AGBe in the docking between the therapeutic targets (Figure 12, 13) presented a higher score for the therapeutic target COX-1, with interactions in important amino acids of this enzyme, with the amide 18: 1, ω-7-ethanolamine, presenting the highest score value, which was 78.40.

Spilantol was used as a standard for comparison because it has a chemical structure similar to AGBe, and because it has anti-inflammatory activity (Wu et al. 2008) and, With the therapeutic target COX-2 (Figure 14), spilantol and 18:2, ω-6-ethanolamine showed interactions, with amino acids with score values of 63.00 and 76.71, respectively, and with the therapeutic target PLA_2 (Figure 15), spilantol had a score value of 62.45 and the 18: 1 molecule, ω-9-ethanolamine had the highest score value and several interactions, in addition to interacting with the two amino acid residues of the active site.

Prostaglandins are derived from arachidonic acid (AA) in a reaction catalyzed by COX, which can exist as COX-1 and COX-2. AA after neopathological stimuli is released from the cell membrane. The inhibitors of this enzyme interfere in this reaction, and, currently, the involvement of COX-1 in cancer and several inflammatory processes is already known (Vitale et al., 2016; Hage Melim et al., 2019).

The RMSD value indicates the accuracy of the docking poses calculated by the GOLD fitting algorithm compared to the poses, determined experimentally, of a compound linked to a biological target. Thus, the calculation of docking with RMSD less than 2 Å for a conformation of fit is considered successful. Therefore, it has justified validity (Cole et al. 2005). Therefore, all AGBe studied had a score value and number of interactions greater than the standard molecule (Spilantol), indicating anti-inflammatory activity related to COX-2 and PLA_2 inhibition.

Carvalho et al. (2017) demonstrated that the administration of an inflammatory agent in the abdominal region of *Danio rerio*, such as carrageenan, can cause reactions in vital organs such as gills, liver, intestine, and kidneys. Borges et al. (2018) stated that the technique of intraperitoneal injection in zebrafish is invasive, which can easily cause damage to the organs contained in the abdominal cavity that is responsible for the metabolism and excretion of various substances.

In the histopathological study, it was observed that the group treated with spilantol (Figure 8) had an IHA of 12.66 for the intestine, considering mild to moderate changes. Souza et al. (2018) described that

spilantol, depending on the dose, can influence the production of histopathological damage in the intestine, liver, and kidneys in zebrafish. In his study, he reported that spilantol caused irreversible damage to the animals' intestines.

In this study, the group treated with AGBe in the highest dose (750 mg/kg) did not present any alterations in Organs evaluated (Figure 9,10 and 11)organs and presented 95% inhibition of the inflammatory process triggered by carrageenan the zebrafish peritoneum (Figure 7B) when compared with the spilantol group. The histopathological study produced considerable changes in the intestine, which is known to have anti-inflammatory activity.

Conclusion

The method used to obtain AGBo from *Bertholletia excelsa* oil was effective and, considering the results obtained in the carrageenan edema test in zebrafish, it can be suggested that AGBe has anti-inflammatory activity including triggering a dose-response effect. The hypothesis of anti-inflammatory action was confirmed in the in silico study, demonstrating the involvement of AGBe in inhibiting the enzymes COX-2 and PLA2, emphasizing the molecules 18: 1 ω-7-ethanolamine and 18: 1, ω-9-ethanolamine. In the histopathological study, AGBe did not cause significant changes in the main metabolizing organs (liver, kidneys, and intestines), while spilantol produced mild to moderate changes in intestinal tissue. Therefore, based on all the results obtained and the fact that until the dose of 1000 mg/kg, orally, in zebrafish, it was not possible to determine the LD50, it can be said that AGBe is effective and safe for the activity anti-inflammatory.

Declarations

Acknowledgment

The authors would like to thank the PAEC OEA / GCUB Program No. 001/2018, under the Cooperation Agreement between the Organization of American States (OAS) and the Coimbra Group of Brazilian Universities (CGUB), for the financial support for student YFQU.

Author contributions

BR carried out the obtaining and characterization of AGBe under the guidance of IMF. In vivo biological assays were performed by YFQU and SFB under GCS, BLSO, and RSB. LISHM carried out the *in silico* study, and JCTC participated as general coordinator of the study and reviewer of the data obtained.

References

Araújo Pedro H. F, Pedro H da S Barata, Inana F Araújo, Jhone M. Curti, Raquel R. Amaral, Didier Berea, José Carlos T. Carvalho, Irlon M. Ferreira (2018) Direct and Solvent-Free Aminolysis of Triglyceride from Oenocarpus bataua (Patawa) Oil Catalyzed by Al2O3. Catalysis Letters 148: 843–851.

Barata Pedro H. S., Ícaro R. Sarquis, Helison DE O. Carvalho, Albenise S. Barros, Alex B. Rodrigues, Adan J. galue-Parra, Edilene O. Silva, José Carlos T Carvalho, Irlon M Ferreira (2020) Chemoenzymatic Synthesis and Anti-Inflammatory Activity of Fatty Acid Amides Prepared from Bertholletia excelsa (Brazil Nut) Triglycerides. J. Braz. Chem. Soc 1: 1-9.

Barbosa, Alan F. Spilantol: occurrence, extraction, chemistry and biological activities (2015). Revista Brasileira De Farmacognosia Rio de Janeiro. 25: 128-133.

Borges, R.S, Keita, H, Ortiz, B.L.S. et al. (2018) Anti-inflammatory activity of nanoemulsions of essential oil from Rosmarinus officinalis L: in vitro and in zebrafish studies. Inflammopharmacol 26: 1057-1080.

Borges, R.S; Lima, E.S.; Keita, H.; Ferreira, I. M.; Fernandes, C. P.; Cruz, R. A. S.; Duarte, J. L.; Velázquez-Moyado, J.; Ortiz, B. L. S.; Castro, A. N.; Ferreira, J. V.; Hage-Melim, L. I. S.; Carvalho, J. C. T (2017) Anti-inflammatory and antialgic actions of a nanoemulsion of Rosmarinus officinalis L. essential oil and a molecular docking study of its major chemical constituents. Inflammopharmacology 26: 183-195.

Borges, Raphaelle Sousa, Brenda Lorena Sánchez Ortiz, Arlindo César Matias Pereiraa , Hady Keitaa,C , José Carlos Tavares Carvalho (2017) Rosmarinus officinalis essential oil: A review of its phytochemistry, antiinflammatory activity, and mechanisms of action involved. Journal of Ethnopharmacology 229: 29-45.

Burgan Sylvia (2016) the zebrafish as a model to study intestinal inflammation. Developmental and Comparative Immunology. Netherlands 64: 1-11.

Carvalho José Carlos Tavares (2017) Fitoterápicos Anti-inflamatórios. Aspectos químicos, farmacológicos e aplicações terapêuticas, 2da edição Pharmabooks, Brasil, págs. 35-51.

Carvalho, J.C. T., Keita, H., Santana, G.R., Souza, G.C., Santos, I.V.F., Amado, J.R., Kourouma, A., Prada, A. L., Carvalho, H. O., Silva, M. L. (2017). Efeitos do veneno de Bothrops alternatus no peixe-zebra: estudo histopatológico. Inflammopharmacology 25: 1–12.

Carnovali M., R. Ottria, S. Pasqualetti, G. Banfi, P. Ciuffreda, M. Mariotti (2016). Effects of bioactive fatty acid amide derivatives in zebrafish scale model of bone metabolism and disease, Pharmacological Research, 104:1-8. DOI: 10.1016/j.phrs.2015.12.009. https:// doi.org/10.1016/j.phrs.2015.12.009

Chakraborty A., B. Devi, R. Sanjebam, S. Khumbong E I. Thokchom (2010) “Estudos preliminares sobre as atividades anestésicas e antipiréticas locais de Spilanthes acmella Murr em modelos animais experimentais, Indian J. Pharmacol 42: 277.

Chandak, N, Kumar, P, Kaushik, P, Varshney, P, Sharma, C, Kaushik, D, Jain, S, Aneja, K. R, Sharma, P. K (2014) Dual evaluation of some novel 2-amino-substituted coumarinylthiazoles as anti-inflammatory–antimicrobial agents and their docking studies with COX-1/COX-2 active sites. Journal of Enzyme Inhibition and Medicinal Chemistry 29(4): 476–484.

Chunhieng, Thavarith; Abdel hafidi; Daniel Pioch; José Brochier; Didier Montet (2008) Detailed study of Brazil nut (*Bertholletia excelsa*) oil micro-compounds: phospholipids, tocopherols and sterols. Journal of the Brazilian chemical society 19(7).

Cole, S.H., Carney, G.E., McClung, C.A., Willard, S.S., Taylor, B.J., Hirsh, J. (2005). Two functional but noncomplementing. Drosophila tyrosine decarboxylase genes. J. Biol. Chem. 280(15):14948-14955.

Collymore, C., Rasmussen, S., Tolwani, R. J (2013) Gavaging Adult Zebrafish. J. Vis.

Da silva, Marcia De Oliveira (2013) atividade farmacológica e toxicológica das flores de *Acmella Oleracea* (L.) R.K. Jansen. Dissertação (Mestrado em recursos naturais da Amazônia) - Universidade Federal do Oeste do Pará.

Dias, A.M.A (2011) Spilantol from Spilanthes acmella flowers, leaves and stems obtained by selective supercritical carbon dioxide extraction. The Journal of Supercritical Fluids 61:1-9.

Dos Santos, Sabrina Matias (2015). Obtenção de spilantol a partir das folhas de jambu (spilanthes acmella (l.) murr. Grau de Bacharel, Universidade Federal do Ceará.

Du, Xing Y., Xia, Y. L., Ai, S. M., Liang, J., Sang, P., Liu, S. Q (2016) Insights into protein–ligand interactions: mechanisms, models, and methods. International journal of molecular sciences 17(2): 144.

Fiorucci, S., Meli, R., Bucci, M., And Cirino, G (2001) Dual inhibitors of cyclooxygenase and 5-lipoxygenase. A new avenue in anti-inflammatory therapy? Biochem. Pharmacol 62:1433–1438.

García De Lorenzo, A Y Mateos, J. López Martínez Y M. Sánchez Castilla (2000) Respuesta inflamatoria sistémica: fisiopatología y mediadores. Medicina Intensiva 24: 8.

Giordanetto, f. Pettersen, D.; Starke, I.; Nordberg, P.; Dahlström, M.; Knerr, L.; Selmi, N.; Rosengren, B.; Larsson, L-O.; Sandmark, J.; Castaldo, M.; Dekker, N.; Karlsson, U.; Hurt-Camejo, E (2016) Discovery of AZD2716: A Novel Secreted Phospholipase A2 (sPLA2) Inhibitor for the Treatment of Coronary Artery Disease. ACS Med. Chem. Lett 7(10): 884-889.

Hage-Melim, L. I. S, Poiani, J. G. C, Da Silva, C. H. T. P (2019) Boylan, F. In silico study of the mechanism of action, pharmacokinetic and toxicological properties of some N-methylanthranilates and their analogs. Food Chem Toxicol 131.

Hernández, I., Márquez, L., Martínez, I., Dieguez, R., Delporte, C., Prietoa, S., Molina Torres, J., Garrido, G (2009). Anti-inflammatory effects of ethanolic extract and alkamides-derived from Heliopsis longipes roots. J. Ethnopharmacol 124: 649–652.

Hsu, S. Da, Chu, C.H., Tsou, A.P., Chen, S.J., Chen, H.C., Hsu, P.W.C., Wong, Y.H., Chen, Y.H., Chen, G.H., Huang, H. DA (2007) miRNAMap 2.0: Genomic maps of microRNAs in metazoan genomes. Nucleic Acids. Published online 36: 165–169.

Huang S-Y, Feng C-W, Hung H-C, Chakraborty C, Chen C-H, Chen W-F, et al. (2014) A Novel Zebrafish Model to Provide Mechanistic Insights into the Inflammatory Events in Carrageenan-Induced Abdominal Edema. PLoS ONE 9(8): e104414. https://doi.org/10.1371/journal.pone.0104414

Kettleborough Ross N W, Elisabeth M Busch-nentwich et al. (2013) A systematic genome-wide analysis of zebrafish protein-coding gene function. Nature 496: 494–497.

Leary S, Anthony R, Cartner S, Corey D, Grandin T, Greenacre C, Gwaltney-Brant S, Mccrackin MA, Meyer R, Miller D, Shearer J, Yanong R (2013) Avma Orientações para a Eutanásia dos Animais.

Li, Y.-C, Chiang, C.-W, Yeh, H.-C, Hsu, P.-Y, Whitby, F. G, Wang, L.-H, Chan, N.-L (2008) Structures of Prostacyclin Synthase and Its Complexes with Substrate Analog and Inhibitor Reveal a Ligand-specific Heme Conformation Change. Journal of Biological Chemistry 283(5): 2917–2926.

Mathur P, Lau B, Guo S. (2011) Conditioned place preference behavior in zebrafish Nat Protoc, 6: 338–345.

Molina-Torres J, Salgado-Garciglia R, Ramirez-Chanez E And del Rio RE (1996), Purelyolefinic alkamides in Heliopsis longipes and Acmella (Spilanthes) oppositifolia. Biochem. Syst. Ecol. 24: 27–43.

Motta, E.V.S.1; Pinto, N.C.C.1; Duque, A.P.N.1; Mendes, R. F.1; Bellozl, P.M.Q.1; Scio, E.1 (2013) Atividades antioxidante, antinociceptiva e anti- inflamatória das folhas de Mucuna pruriens (L.) DC. Revista Brasileira de Plantas Medicinais 15: 264-272.

Muniz Marcos Antônio Pena, Marina Nídia Ferreira dos Santos, Carlos Emmerson Ferreira Da Costa, Luiz Morais, Maria Louze Nobre Lamarão, Roseane Maria Ribeiro-Costa, José Otávio Carréra Silva-Júnior (2015) Physicochemical characterization, fatty acid composition, and thermal analysis of Bertholletia excelsa HBK oil. Pharmacognosy Magazine, 11:1-6.

Orlando, B. J.; Malkowski, M. G (2016) Substrate-selective Inhibition of Cyclooxygenase-2 by Fenamic Acid Derivatives Is Dependent on Peroxide Tone. Journal of Biological Chemistry, 291(29): 15069–15081.

Peterson, R. T, Macrae, C A. (2015) Zebrafish as tools for drug discovery. Nature Reviews. Drug discovery, 14: 721-731.

Ribeiro, L. C. (2013.) Investigação do efeito ictiotóxico do extrato etanolico da raiz de Spilanthes acmella (jambu) em zebrafish através da análise eletrofisiológica e comportamental. Dissertação (Mestrado em Neurociências e Biologia) Instituto de Ciências Biológicas, Universidade Federal do Pará-Belém.

Sandy, M.; Butler, A. (2009) Microbial Iron Acquisition: Marine and Terrestrial Siderophores. Chemical Reviews, 109(10): 4580–4595.

Schmidt, R; Strähle, U. (2013) Scholpp, S. Neurogenesis in zebrafish – from embryo to adult. Neural development. 8:3.

Shawahna, R., Jaradat, NA (2017) Ethnopharmacological survey of medicinal plants used by patients with psoriasis in the West Bank of Palestine. BMC Complement Altern Med. 17(1). https://doi.org/10.1186/s12906-016-1503-4

Souza, G. C., Duarte, J. L., Fernandes, C. P., Moyado, J. A. V., Navarrete, A., Carvalho, J. C. T. (2016) Obtainment and study of the toxicity of perillyl alcohol nanoemulsion on zebrafish (*Danio rerio*). J Nanomed Res, 4:93.

Souza, Gisele Custódio De, Md Viana, Ldm Goe´s, Bl Sanchez-Ortiz, Ga Da Silva , Wb De Souza Pinheiro, Cb Rodrigues Dos Santos And Jc Tavares Carvalho. (2019) Reproductive toxicity of the hydroethanolic extract of the flowers of acmella oleracea and spilantol in zebrafish: in vivo and in silico evaluation**.** Human & Experimental Toxicology. https://doi:10.1177/0960327119878257

Vitale, P., Panella, A., Scilimati, A., Perrone, M.G. (2016) COX-1 inhibitors: beyond structure toward therapy. Med. Res. Rev. 36: 641–671.

Wu, L. C.; Fan, N. C.; Lin, M. H.; Chu, I. R.; Huang, S. J.; Hu, C. Y.; Han, S. Y. (2008) Anti-inflammatory effect of spilantol from Spilanthes acmella on murine macrophage by down-regulating LPS-induced inflammatory mediators. J Agric Food Chem. 56: 2341-2349.

Zaa, César, Martha Valdivia, y Álvaro Marcelo. (2012). Efecto Antiinflamatorio Y Antioxidante Del Extracto Hidroalcohólico De Petiveria Alliacea. *Revista Peruana De Biología* 19: 329 -34. https://doi.org/10.15381/rpb.v19i3.1049.

Tables

Table. 1 Composition of ethyl ester from samples derived from *Bertholletia excelsa* oil determined by CG-EMa analysis

Fatty acid[b]	Peak (min.)	Fatty Amide corresponding	Relative concentration (%)
Palmitic (C16: 0)	1	*N*-C16:0-ethanolamine	19
Linoleic (C 18: 2 ω-6)	2	*N*-C18:2, -6-ethanolamine	29
Oleic (C 18: 1 ω-9)	3	*N*-C18:1, -9-ethanolamine	32
Vaccine (C 18: 1 ω-7)	4	*N*-C18:1, -7-ethanolamine	2
Stearic (C 18: 0)	5	*N*-C18:0-ethanolamine	17
Not identified	*	-	1
∑ Satured	–	–	36
∑ Unsaturated	–	–	34
∑ Polyunsaturated	–	–	29

[a]MS database (NIST 5.0); [b]% of the fatty acid corresponding to the *Bertholletia excelsa* oil

Figures

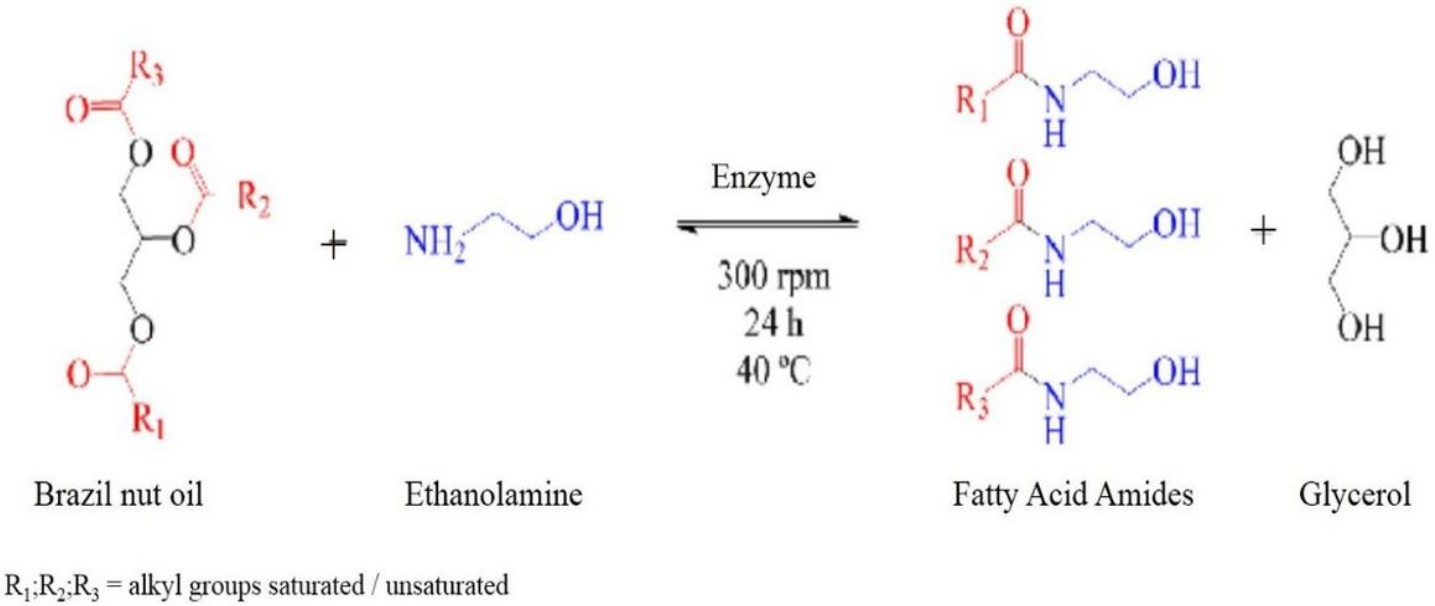

Figure 1

Reaction of aminolysis with Brazil nut oil and ethanolamine.

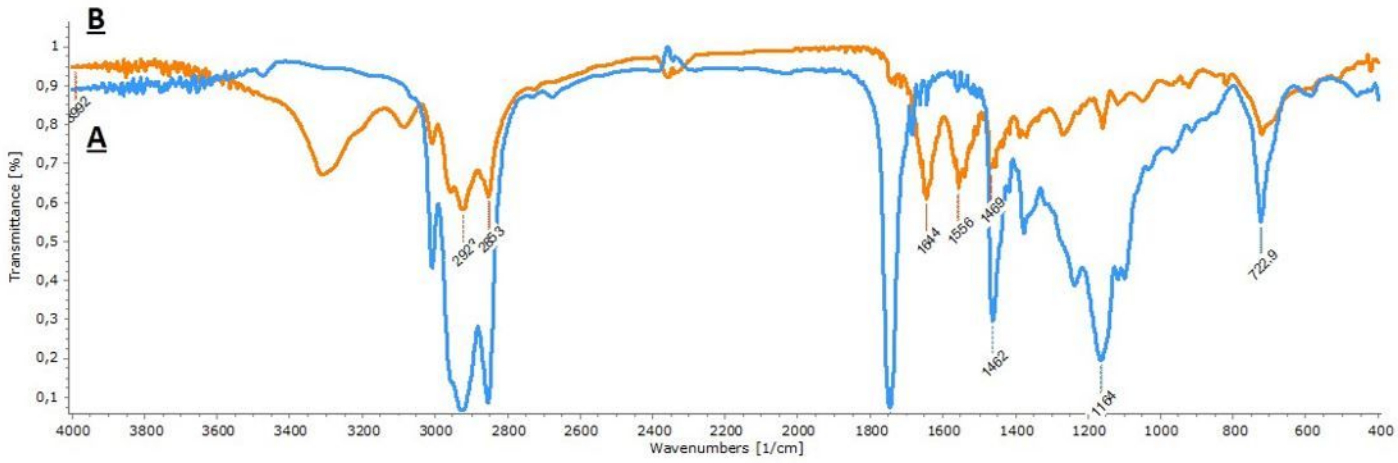

Figure 2

Infrared spectra of the Bertholletia excelsa oil (A) and fatty acid amide (B) compounds.

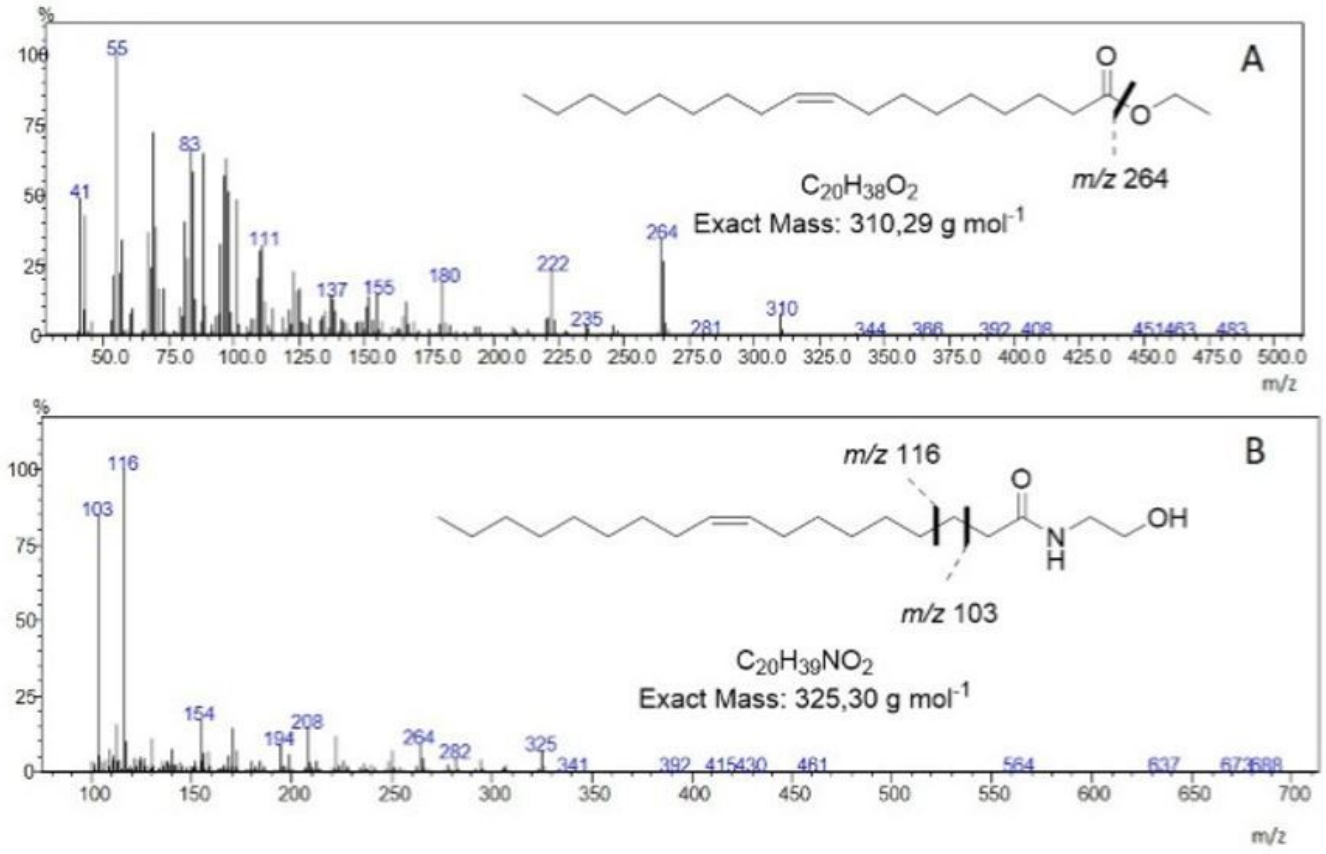

Figure 3

Mass spectra of the ethyl oleate (A) and oleic acid amide (B) compounds

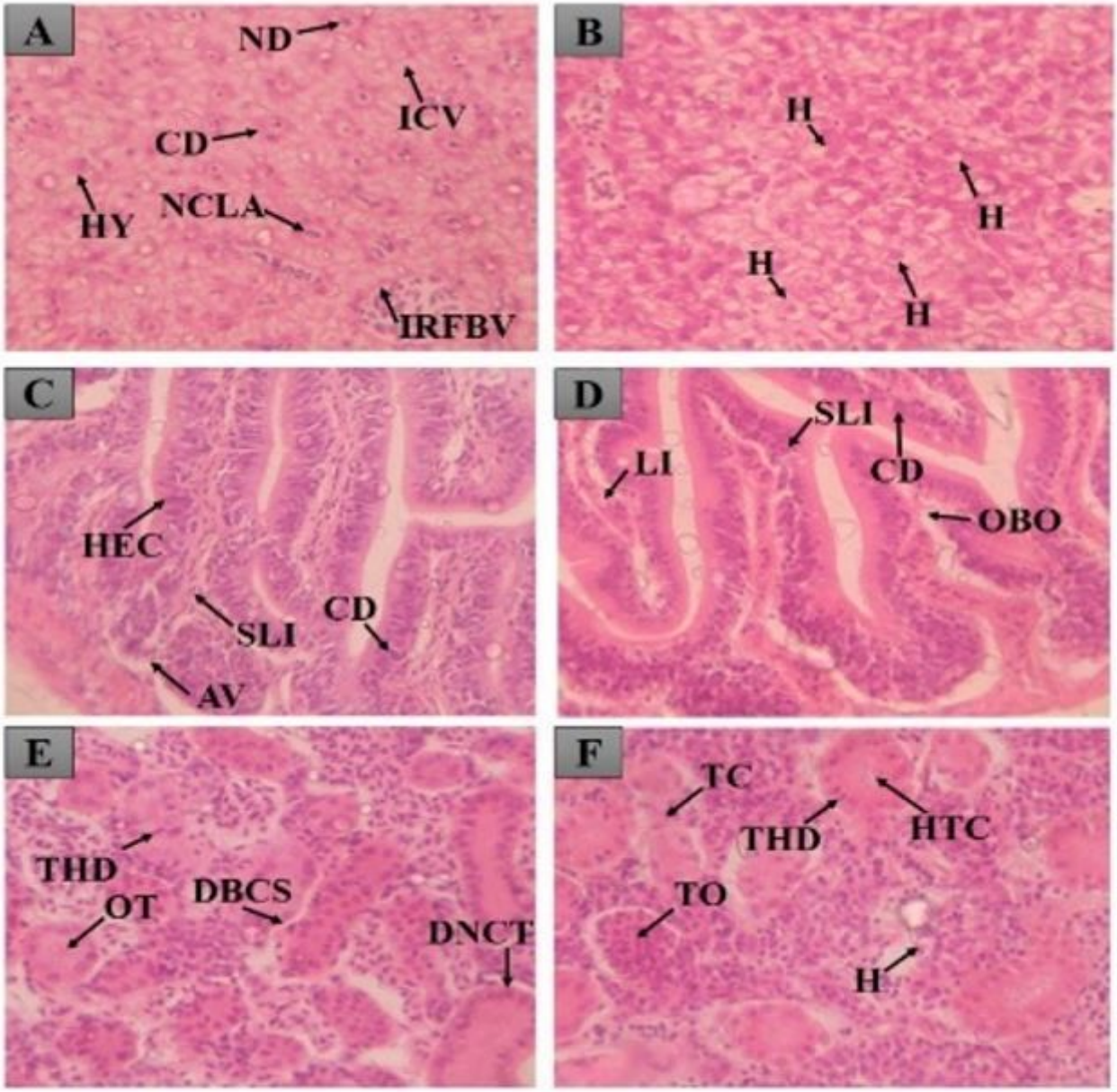

Figure 4

Effect of treatment (single dose) orally with AGBe (1000 mg / kg) and Bertholletia excelsa oil (1000 mg / kg) on Danio rerio's organs (liver, kidneys, intestine). A - Liver, C - Intestine, E - Kidney of animals treated with AGBe. B - Liver D - Intestine F – Kidney of animals treated with Bertholletia excelsa oil.Nuclear degeneration (ND), Cytoplasmic degeneration (DC), intense cytoplasmic vacuolization (ICV), Loss of nuclear contour (NCLA), Hyperemia (HY), Increased relative blood vessel frequency (IRFBV), Epithelial cell hypertrophy (HEC) , Stromal lymphocytic infiltration (SLI), Villus atrophy (AV), Tubular hyaline degeneration (THD), Tubular obstruction (OT), Bowman's capsule space decrease (DBCS), Nuclear tubular cell degeneration (DNCT), Hepatocyte (H), Leukocyte infiltration (LI), Displacement of the lamina propria (OBO), Tubular disorganization (CT), Hypertrophy of tubular cells (HTC), All photos were enlarged by 400x (H & E).

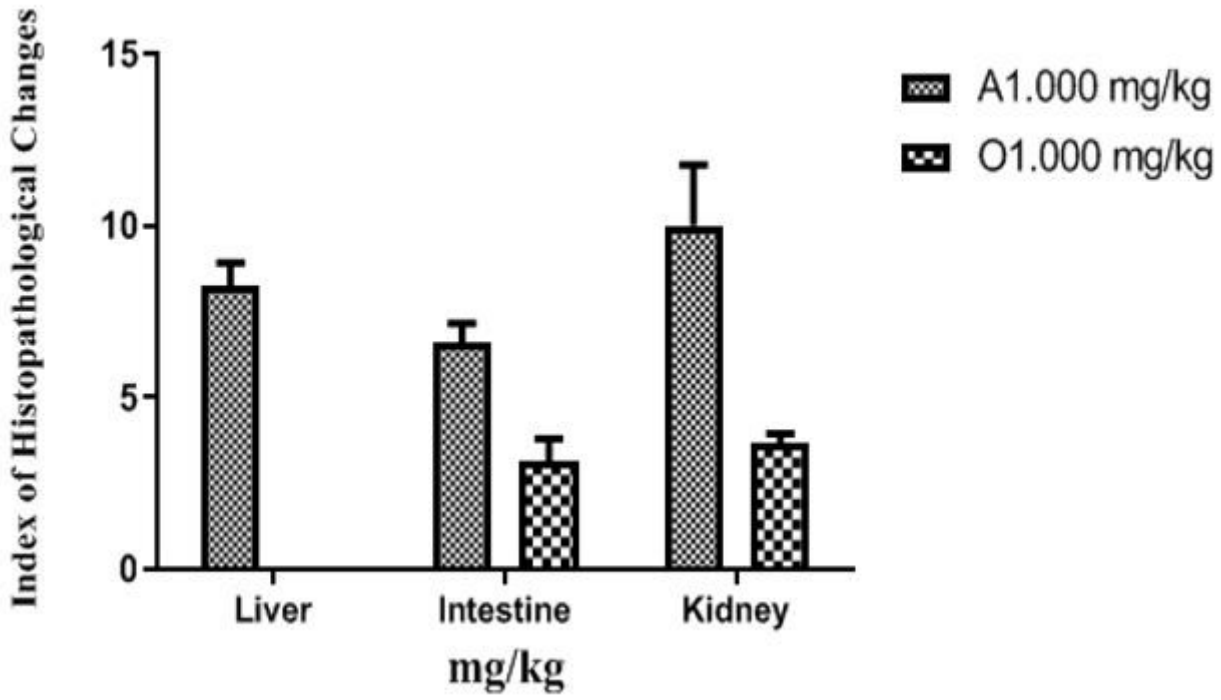

Figure 5

Effect of treatment (single dose) orally with AGBe (A - 1000 mg/kg) and Bertholletia excelsa oil (1000 mg/kg) on the Index of Histopathological Changes for liver, intestine and kidney in Zebrafish in the evaluation of toxicity, observed forty-eight hours after. * $p < 0,05$ (analyzed by ANOVA, followed by the Tukey-Kramer test for comparisons between the treated and control groups), for n = 12/ group.

Figure 6

Effect of oral administration of saline and PBS (SS/PBS, 2µl - A), Tween + DMSO + distilled water 2µl (Thinners - B), Indomethacin (C - 10 mg/kg), spilantol (D - 35 mg/kg), e AGBe (E – F – G - 100 mg/kg, 500 mg/kg and 750 mg/kg) on carrageenan edema (200 µg/animal).

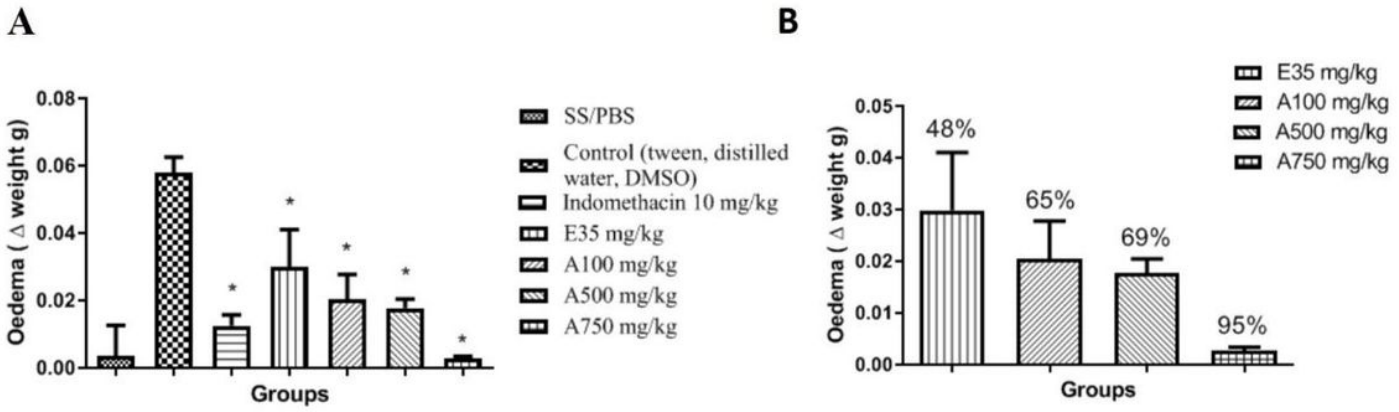

Figure 7

Effect of oral administration of saline and PBS (SS/PBS, 2µl), Tween + DMSO + distilled water 2µl (Thinners), Indomethacin (10 mg/kg), spilantol (E 35 mg/kg), AGBe (A 100 mg/kg, 500 mg/kg and 750 mg/kg) on carrageenan edema (200 µg/animal). * p < 0,05 ANOVA followed by the Tukey test, n = 16.

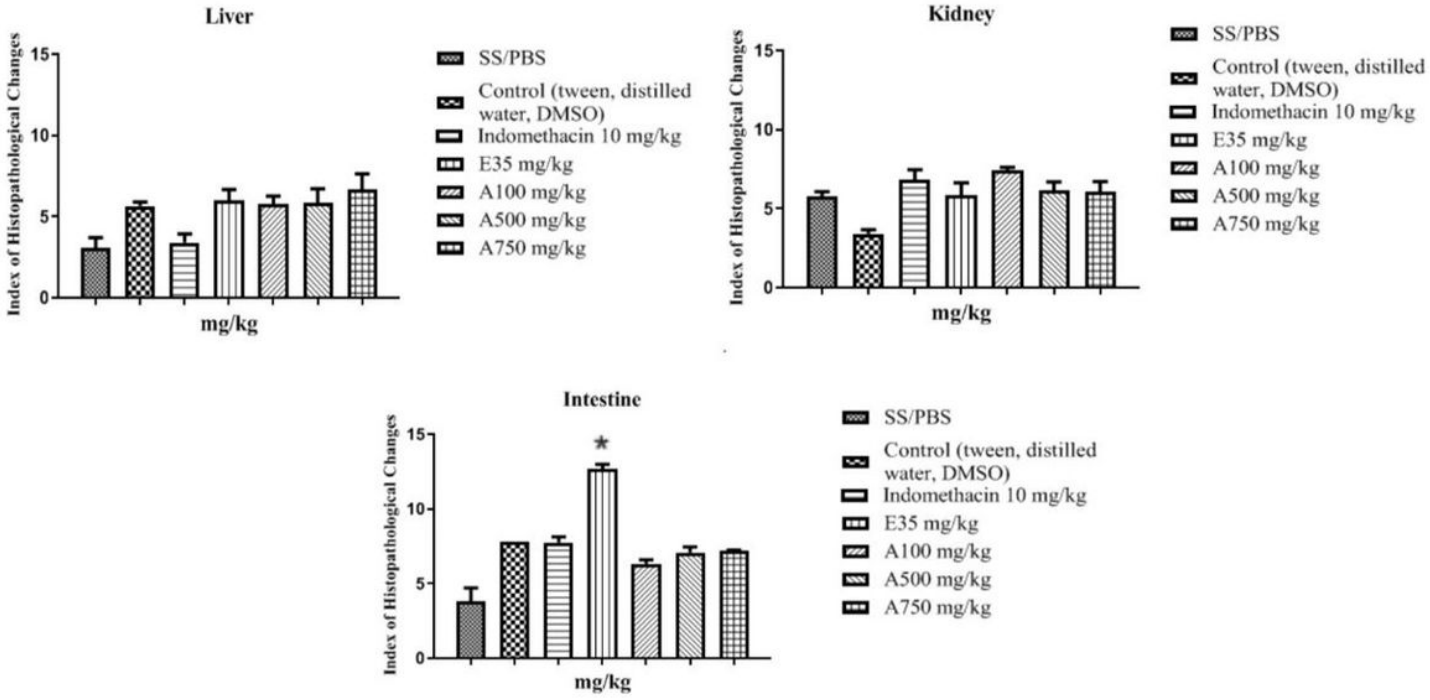

Figure 8

Effect of oral administration of saline and PBS (SS/PBS, 2µl), Tween + DMSO + distilled water 2µl (Thinners), Indomethacin (10 mg/kg), spilantol (35 mg/kg), AGBe (100 mg/kg, 500 mg/kg and 750 mg/kg) on the Index of Histopathological Changes for liver, intestine and kidney in Zebrafish with the application of carrageenan (200 ug/animal).). * p < 0,05 ANOVA followed by the Tukey test, n = 16.

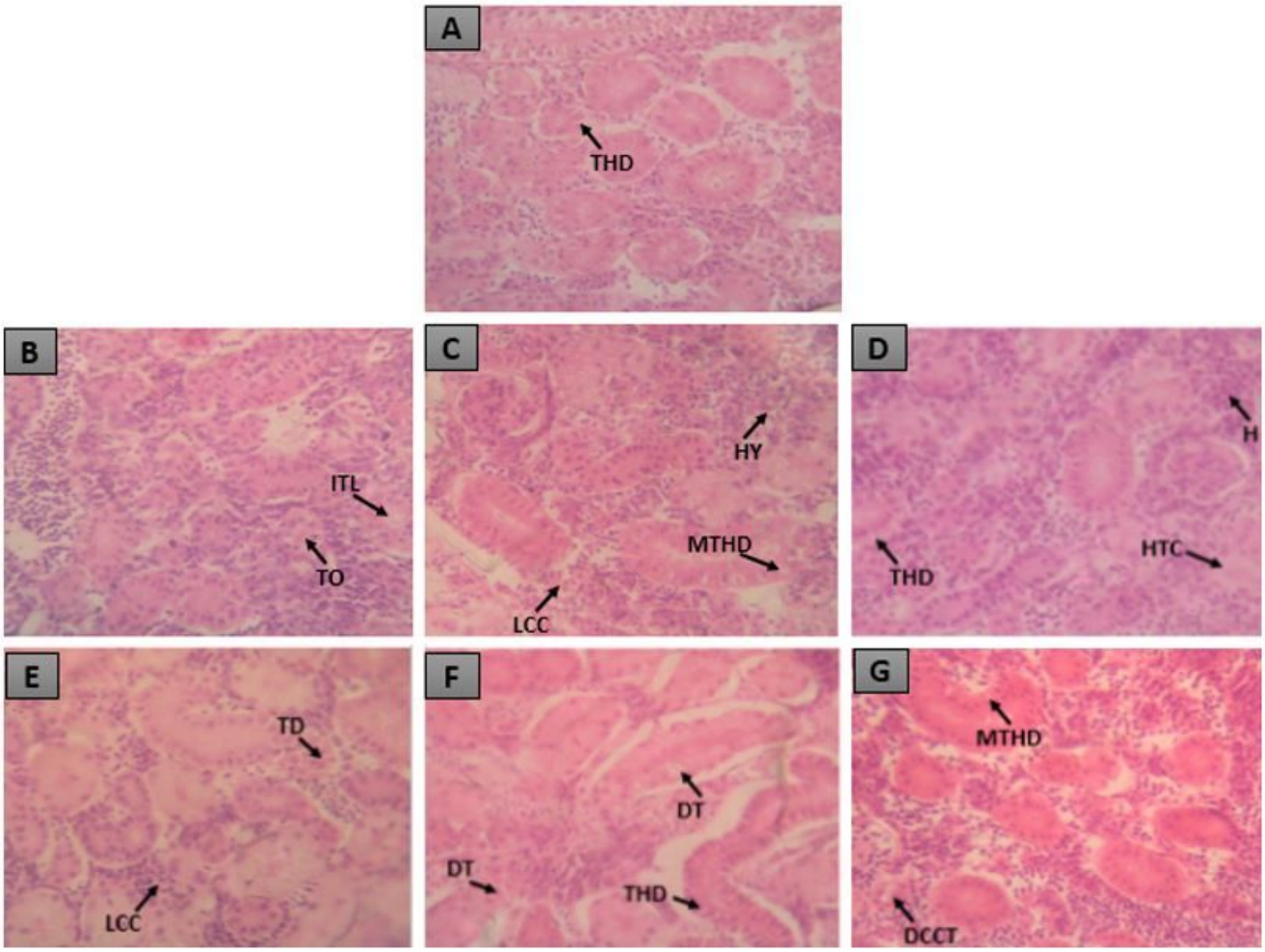

Figure 9

Effect of oral administration of A - Saline solution /PBS; B -Thinners; C– Indomethacin; D- spilantol (35 mg/kg); E, F, G – AGBe (100-500-750 mg/kg) on carrageenan edema (200 µg/animal) in zebrafish. Histopathology of the kidneys. Tubular hyaline degeneration (THD). Increased tubular lumen (ITL), Tubular obstruction (OT), hyperemia (HY), Loss of cell contour (LCC), Tubular degeneration (TD), Cytoplasmic degeneration of tubular cells (DCCT), Hypertrophy of tubular cells (HTC), hyperemia (HY). All photos were enlarged in 400 x (H & E).

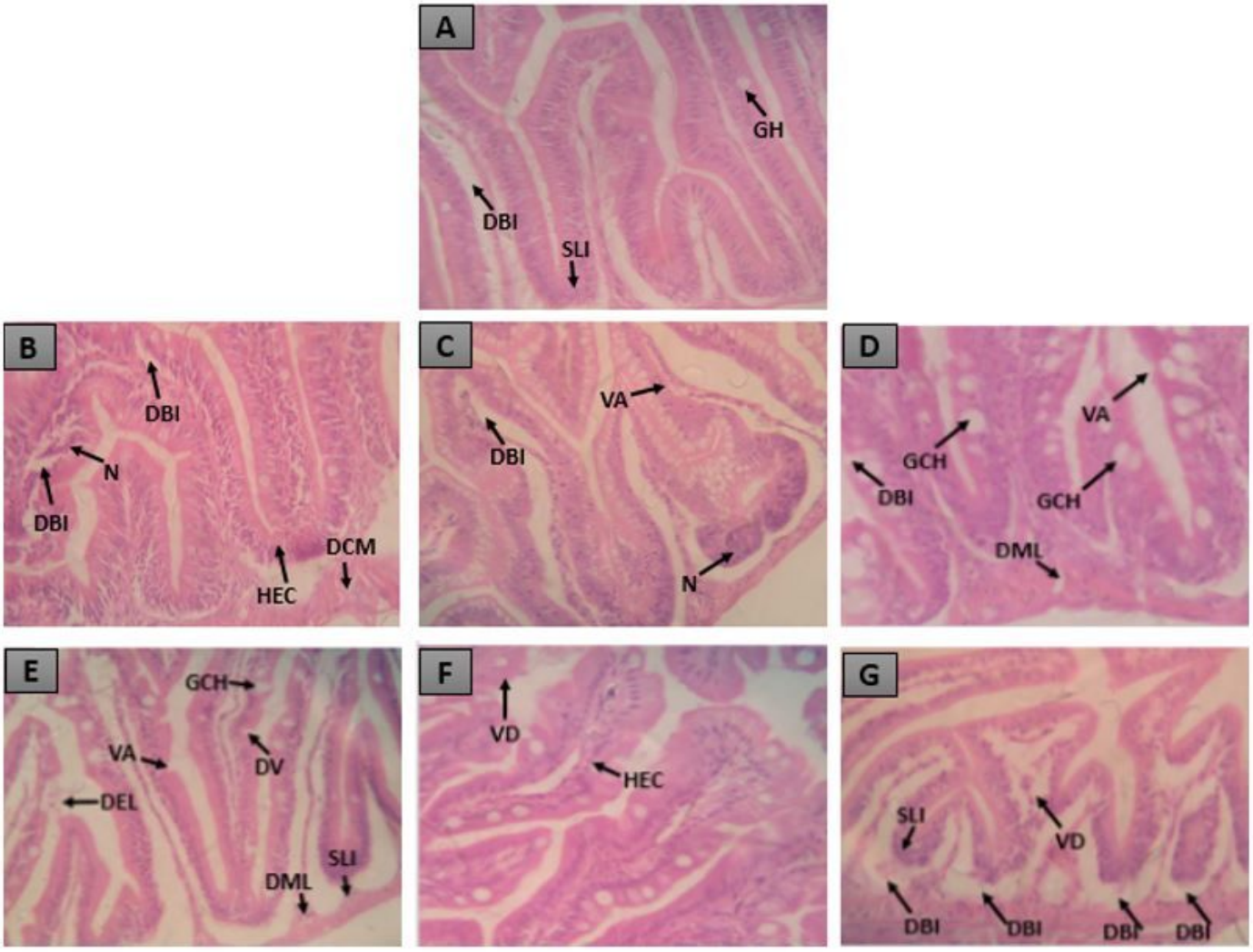

Figure 10

Effect of oral administration of A - Saline solution /PBS; B -Thinners; C– Indomethacin; D- spilantol (35 mg/kg); E, F, G – AGBe (100-500-750 mg/kg) on carrageenan edema (200 µg/animal) in zebrafish. Histopathology of the Intestine. Detachment of lamina propria (DBI), stromal lymphocytic infiltration (SLI), Goblet cell hyperplasia (GH), Necrosis (N), Epithelial cell hypertrophy (HEC), Muscle layer degeneration (DCM), Villus atrophy (VA) , Detachment of the epithelial lining (LED), Goblet cell hyperplasia (GCH), Villous degeneration (RV), Muscle layer degeneration (DML), Stromal lymphocyte infiltration (SLI), Goblet cell hyperplasia (GCH). All photos were enlarged by 400 x (H & E).

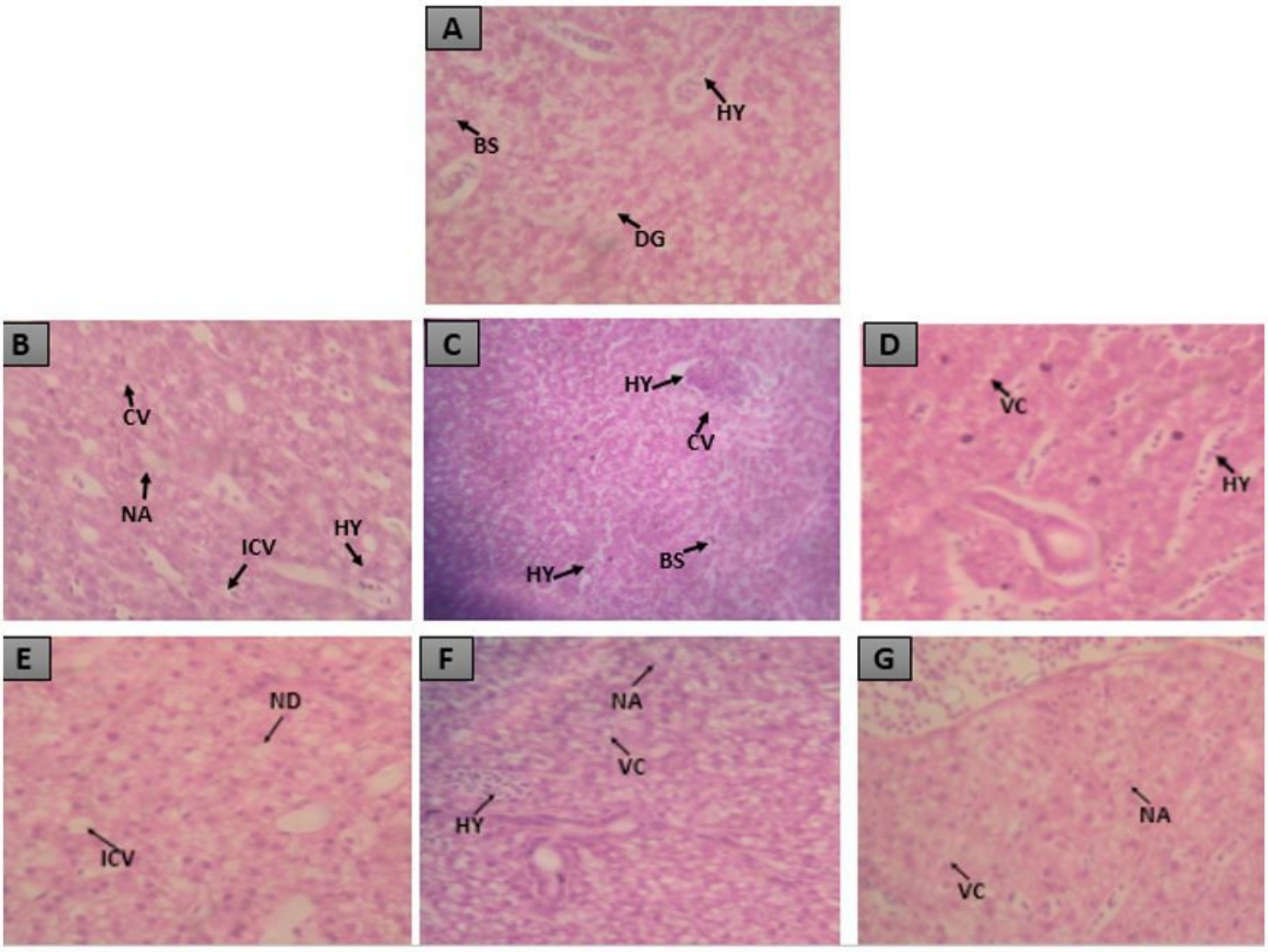

Figure 11

Effect of oral administration of A - Saline solution /PBS; B -Thinners; C– Indomethacin; D- spilantol (35 mg/kg); E, F, G – AGBe (100-500-750 mg/kg) on carrageenan edema (200 ug/animal) in zebrafish. Liver Histopathology. Biliary stagnation (BS), Hyperemia (HY), Decreased glycogen (DG), cytoplasmic vacuolization (CV), Nuclear atrophy (NA), Increased cell volume (ICV), Nuclear degeneration (ND), Nuclear atrophy (NA). All photos were enlarged by 400 x (H & E).

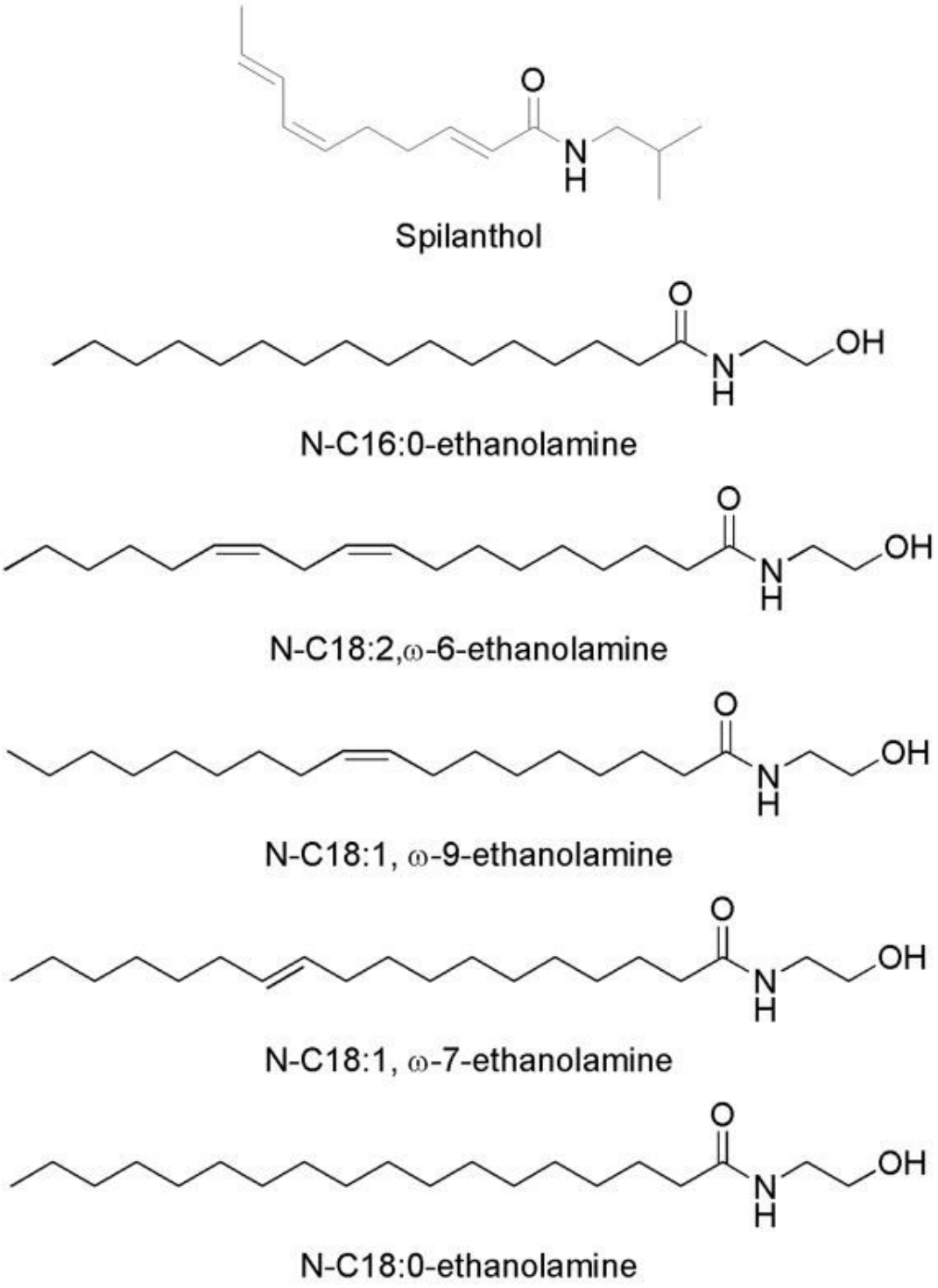

Figure 12

Chemical structure of the studied compounds, Spilantol, 16:0-ethanolamine, 18:2, ω-6-ethanolamine, 18:1, ω-9-ethanolamine, 18:1, ω-7-ethanolamine e 18:0-ethanolamine.

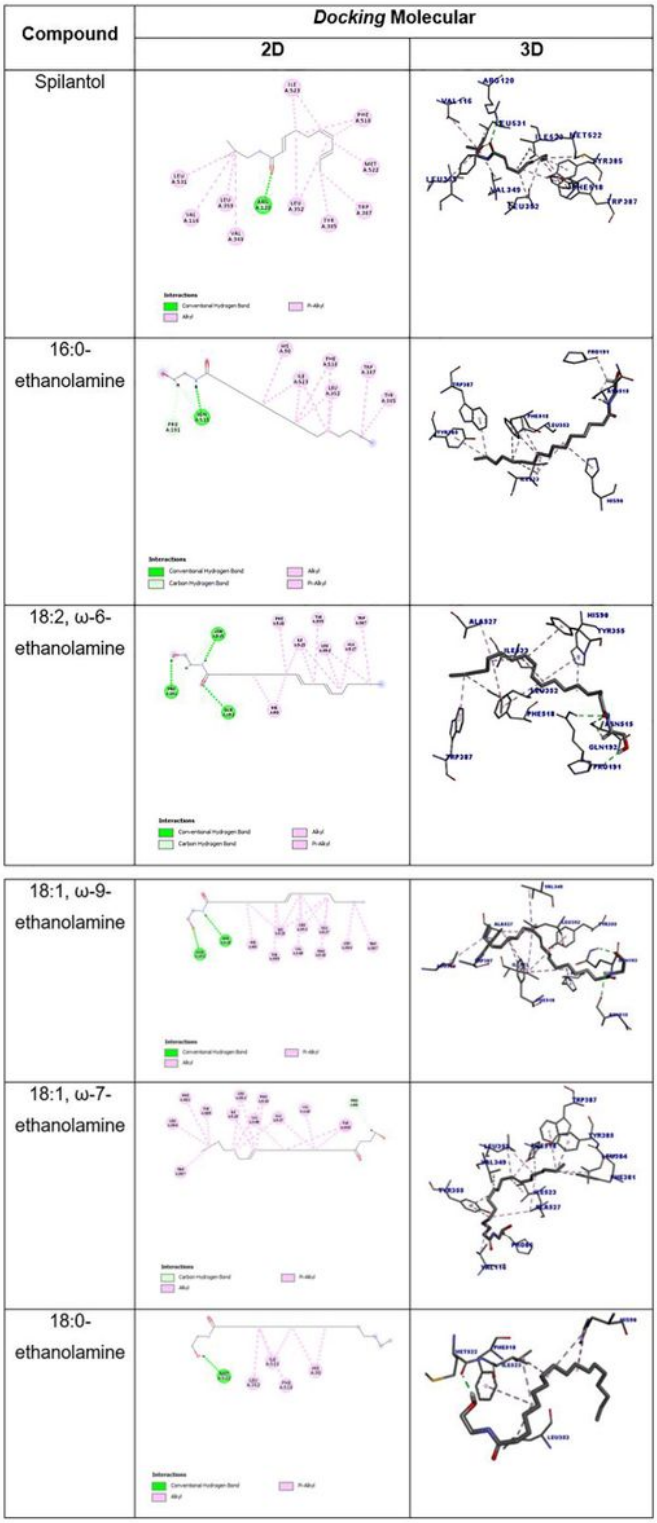

Figure 13

Docking of compounds Spilantol, 16:0-ethanolamine, 18:2, ω-6-ethanolamine, 18:1, ω-9-ethanolamine, 18:1, ω-7-ethanolamine e 18:0-ethanolamine performing interaction with COX-1.

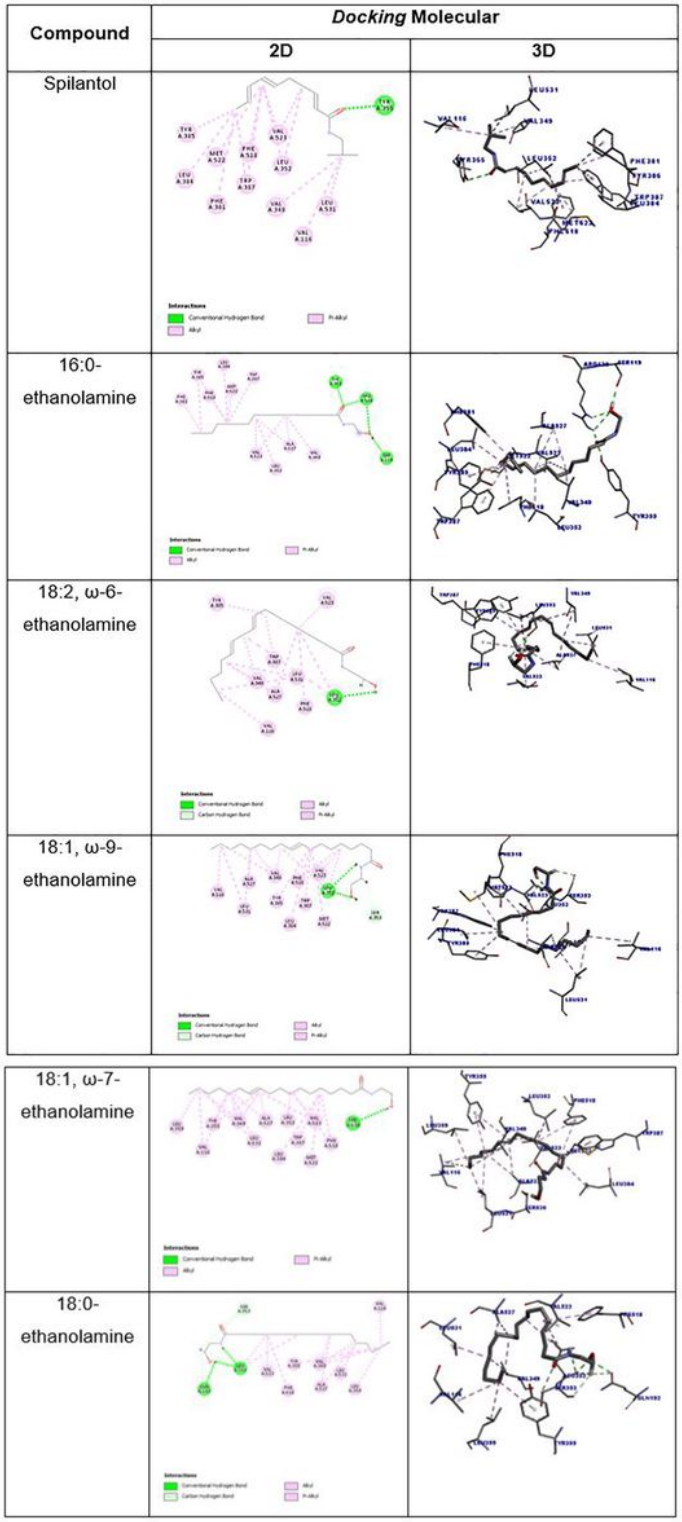

Figure 14

Docking of compounds Spilantol, 16:0-ethanolamine, 18:2, ω-6-ethanolamine, 18:1, ω-9-ethanolamine, 18:1, ω-7-ethanolamine e 18:0-ethanolamine performing interaction with COX-2.

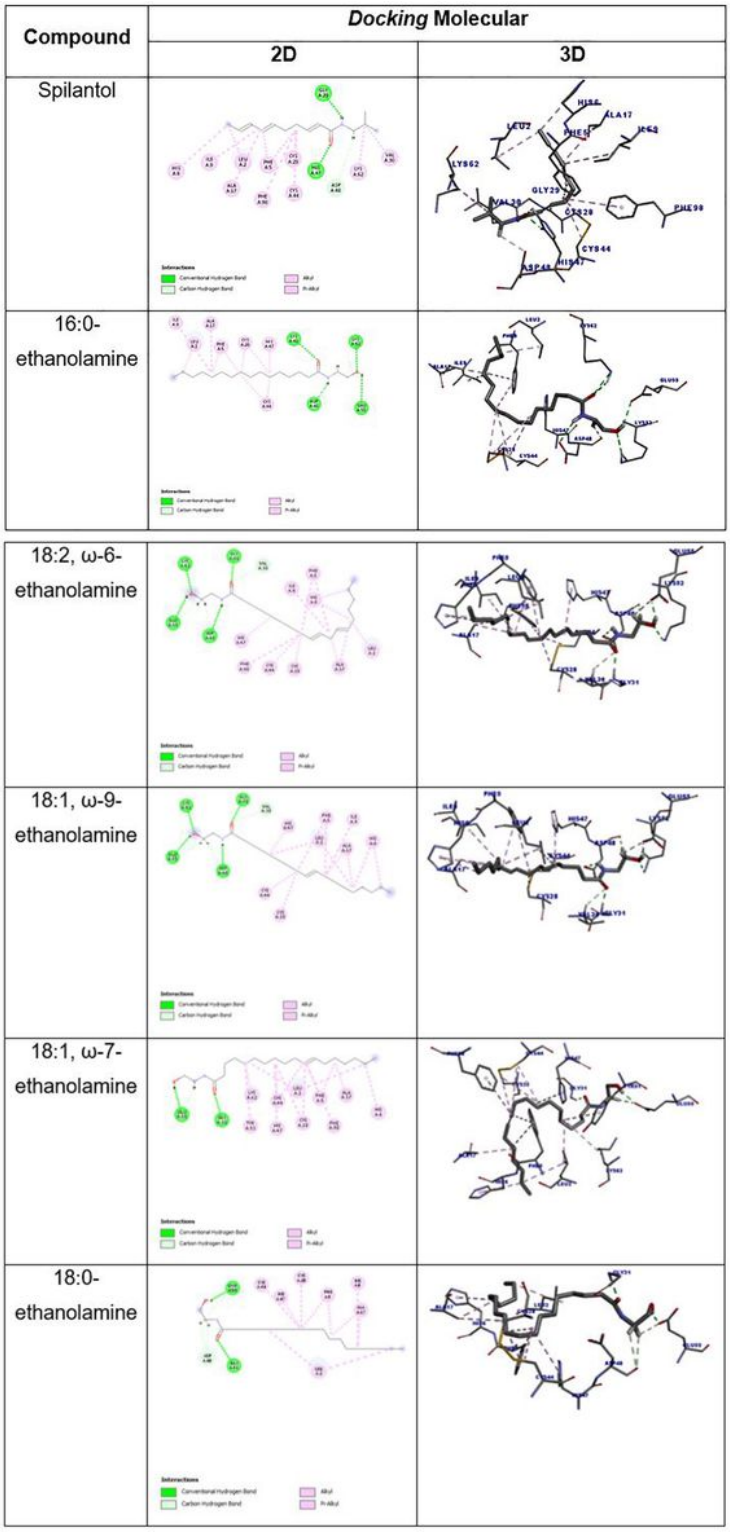

Figure 15

Docking of compounds Spilantol, 16:0-ethanolamine, 18:2, ω-6-ethanolamine, 18:1, ω-9-ethanolamine, 18:1, ω-7-ethanolamine e 18:0-ethanolamine performing interaction with PLA2.